Electronic Supplementary Information

for

Nucleophilic hydrolysis enables HF-etched MXene kilofarad specific capacitance and excellent rate performance

Jiang Xu,[a,b] Yaokai Gu,[a] Bingqing Hu,[a] Haoqi Yang,[b] Dawei Sha,[b] Jiabiao Lian[c,*] and Shanhai Ge[d,*]

[a] School of Mechanical Engineering, Jiangsu University, Zhenjiang 212013, P. R. China.

[b] College of Electrical, Energy and Power Engineering, Yangzhou University, Yangzhou 225127, P. R. China.

[c] Institute for Energy Research, Jiangsu University, Zhenjiang 212013, P. R. China.

[d] Department of Mechanical Engineering, The Pennsylvania State University, University Park, PA 16802, USA.

Corresponding authors:

E-mail: jblian@ujs.edu.cn (J. Lian); sug13@psu.edu (S. Ge).

Experimental Section

Preparation of the pristine $Ti_3C_2T_x$ MXene and hydrothermally treated MXene.

HF-etched $Ti_3C_2T_x$ MXene and hydrothermally treated MXene powders: $Ti_3C_2T_x$ powders were synthesized by etching Ti_3AlC_2 powders (400 mesh; 11 Technology Co., Ltd., P. R. China) with HF as previously reported.[S1] Typically, 1 g of Ti_3AlC_2 powders were slowly added into 10 ml 40 wt.% HF solution (Sinopharm Chemical Reagent Co., Ltd., Shanghai, P. R. China) and stirred at 35°C for 24 h. The resulting powders were vacuum-filtered and washed several times with deionized water. Finally, the product $Ti_3C_2T_x$ powders were dried at 80°C overnight under vacuum. For hydrothermally treated MXene powders, 0.5 g of the pristine $Ti_3C_2T_x$ powders were added into 25 ml 0.5 M KOH solution and transferred into 50 ml para polyphenol (PPL) lined stainless steel autoclave under Ar flow (to remove the air in the lining) and kept at 180, 200, 220, 240, and 260°C for 10 h, respectively. After cooling down to room temperature, the product was washed with 1 M H_2SO_4 and then deionized water by centrifuging until the pH of the solution reached about 6. Finally, the sediments were vacuum dried at 80°C overnight, and the products were denoted as H-T (T represents hydrothermal temperature).

HCl+LiF-etched $Ti_3C_2T_x$ MXene and hydrothermally treated MXene colloidal solution: A mixture of HCl and LiF was used to synthesize multilayer $Ti_3C_2T_x$ from Ti_3AlC_2 powder, similar to the method reported in our previous study.[S2] In detail, 1 g of LiF (Sinopharm Chemical Reagent Co., Ltd., Shanghai, P. R. China) was added into 20 ml of 9 M HCl solution, followed by a slow addition of 1 g Ti_3AlC_2 powders with stirring in ice bath, and then transferred to oil bath. After etching for 36 h at 40°C, the product was washed with deionized water by centrifuging until the pH of the supernatant reached about 6. The remained sediment (multilayer $Ti_3C_2T_x$) was mixed with 100 ml deionized water and probe sonicated (power: 400 W) for 1 h under Ar atmosphere and ice bath. Afterward, the mixture was centrifuged for 1 h at 3500 rpm. The resultant dark supernatant was a colloidal solution of few-layer $Ti_3C_2T_x$. The concentrated colloidal $Ti_3C_2T_x$ solution was diluted to 2 mg ml^{-1}. Next, 1.5 g KOH was slowly added into 35 ml of the diluted $Ti_3C_2T_x$ colloidal solution. The resultant suspension was transferred into

50 ml para polyphenol (PPL) lined stainless steel autoclave purged with Ar at a flow rate of 200 ml min^{-1} for 5 minutes (to remove the air and dissolved oxygen in the lining, the presence of oxidants will lead to the oxidation of MXene and form Na/K-titanates after hydrothermal treatment in NaOH/KOH solution[S3,S4]) and kept at 220°C for 10 h. After cooling down to room temperature, the product was washed with 1 M H_2SO_4 and then deionized water by centrifuging until the pH of the supernatant reached about 6. The remained sediment was mixed with 100 mL deionized water and probe sonicated (power: 400 W) for 20 min under an Ar atmosphere and in an ice bath to obtain a hydrothermally treated MXene colloidal solution.

Preparation of chemically pre-protonated Turnbull's blue analogue (H-TBA): H-TBA was synthesized by chemical reduction of $Cu^{II}[Fe^{III}(CN)_6]_{2/3}\cdot 4H_2O$ (denoted as CuFe-TBA).[S5] For the CuFe-TBA synthesis, 50 ml of 0.2 M $CuSO_4$ solution was added dropwise into 50 ml of 0.1 M $K_3Fe(CN)_6$ solution under magnetic stirring. After reacting for 6 hours, the resulting olive-green precipitate was washed with deionized water and centrifuged 8 times, then dried in an oven at 60°C overnight. For the chemical reduction, the as-prepared powder (0.4 g) was dispersed in 40 ml of deionized water and sonicated for 30 min. Under Ar bubbling and stirring conditions, 20 ml of 0.05 M hydrazine solution was added dropwise to the above powder suspension. After reacting for 2 hours, the crimson precipitate was washed and centrifuged 8 times, then dried in a vacuum oven overnight (40°C) to obtain H-TBA powder.

Characterizations.

The phase of the samples was confirmed by the powder X-ray diffractometer (Bruker D8 advance powder diffractometer equipped with copper Kα radiation, λ=1.5418 Å). Morphology observations were performed on a field emission scanning electron microscope (FE-SEM, JEOL JSM-7800F) equipped with an energy-dispersive X-ray spectroscope (EDS, Oxford), transmission electron microscopy (TEM, FEI Talos F200x G2). The chemical compositions of the samples were further analyzed by ESCALAB 250Xi X-ray photoelectron spectroscopy (XPS, Thermo Fisher Scientific). Peak fitting was carried out by using Thermo Avantage software.

Electrode preparation.

In this work, the activated carbon (AC) electrode was used as counter electrode and prepared by mechanical processing of a pre-mixed slurry, containing 90 wt.% YP-50 AC (Kuraray, Japan), 5 wt.% Ketjen black (ECP600JD, Lion Specialty Chemicals Co., Ltd.) and 5 wt.% polytetrafluoroethylene (PTFE, 60 wt.% in water, DAIKIN, Japan) binder in ethanol. The mass loading of the obtained electrode was set at ~15 mg cm^{-2}. For the HCl+LiF-etched film electrode, $Ti_3C_2T_x$ colloidal solution was vacuum filtered through a 25 μm thick Celgard 3501 polypropylene membrane. The wet film on the Celgard membrane was collected and dried in vacuum overnight at 80°C. Afterwards, a flexible, freestanding $Ti_3C_2T_x$ thin film was collected by peeling the thin film off the Celgard membrane. HF-etched $Ti_3C_2T_x$ electrode was prepared by mechanical processing of a pre-mixed slurry, containing 95 wt.% HF-etched $Ti_3C_2T_x$ (or hydrothermally treated powders) and 5 wt.% PTFE binder in ethanol. The mass loading of the electrode was set at ~4 mg cm^{-2}. For the H-TBA electrode, a mixture slurry containing 70 wt.% H-TBA powder, 20 wt.% Ketjen carbon, and 10 wt.% polyvinylidene fluoride binder (PVDF, Solvay (Shanghai) Co., Ltd.) was coated on a carbon fiber paper current collector to serve as a cathode.

Electrochemical setup and tests.

All electrochemical tests in aqueous electrolytes were performed in three-electrode Swagelok cells using glass carbon as a current collector. Ag/AgCl in saturated KCl solution and Celgard 3501 membrane were used as the reference electrode and separator, respectively. For two-dimensional $Ti_3C_2T_x$ MXene, besides intercalation capacitance between 2D $Ti_3C_2T_x$ layers, -O terminal functional groups formed on the surface of Ti_3C_2 could provide pseudo-capacitance due to the similarity to transition metal oxides. In addition, to avoid the reduction of water, only hydrogen ion (H^+) could react with Ti-O in a suitable potential window when using $Ti_3C_2T_x$ as an anode. Compared with other acids, sulphuric acid is not volatile and has high conductivity, which has been widely used as electrolyte in lead-acid batteries. Herein, 5 M H_2SO_4 was used as electrolyte. Cyclic voltammetry, galvanostatic charge-discharge (GCD), and electrochemical impedance spectroscopy were performed on CHI660E

electrochemical workstation. After initially pre-cycling the electrode 40 times at 5 mV s^{-1}, cyclic voltammetry was performed with scan rates from 2 to 100 mV s^{-1}. GCD was performed with current densities ranging from 5 to 100 A g^{-1}. Additionally, a cycling life test was performed at a current density of 100 A g^{-1} for 10,000 cycles.

To validate the adaptability of MXene for practical applications, a proton battery was fabricated and investigated. Here, H-220 and H-TBA were used as the anode and cathode, respectively. Considering the capacity matching of the anode and cathode, the mass loadings of H-220 and H-TBA were set as 2 and 5 mg cm^{-2}, respectively. All tests (including CV, GCD, and cycling life) were performed in Swagelok cells.

Calculations for the electrochemical tests.

The specific capacitance (C_{CV}, F g^{-1}) of a single electrode is evaluated from the anodic scan of the CV curves based on

$$C_{CV}\ (\mathrm{F\ g^{-1}}) = \frac{\int i dU}{mvU} \quad (1)$$

where i and v are the charging current (A) and the scan rate (V s^{-1}), respectively, m is the mass (g) of a single electrode, and U is the potential window (V).

For the GCD curve, the specific capacitance (C_{GCD}, F g^{-1}) of a single electrode is evaluated using

$$C_{GCD}\ (\mathrm{F\ g^{-1}}) = \frac{I\,\Delta t}{mU} \quad (2)$$

where I (A) is the constant current applied to the cell, Δt (s) is the charge/discharging time, m (g) is the active mass of a single electrode, and U is the potential window (V).

For the two-electrode cell, the specific capacity ($Q_{GCD,\ full\ cell}$, mAh g^{-1}) of the full cell was evaluated based on the GCD curve:

$$Q_{GCD,\ full\ cell}\ (\mathrm{mAh\ g^{-1}}) = \frac{I\,\Delta t}{3.6 m_{total}} \quad (3)$$

where m_{total} is the total mass of active materials on both electrodes.

The specific energy (E_{GCD}, Wh kg^{-1}) of the full cell was estimated based on the

discharge branch of the GCD curve:

$$E_{GCD}\ (\mathrm{Wh\ kg^{-1}}) = \frac{I\left(\int_{V_0}^{V_{max}} t\mathrm{d}V\right)}{3.6m_{total}} \quad (4)$$

where V_0 to V_{max} is the voltage window of the full cell.

Figures

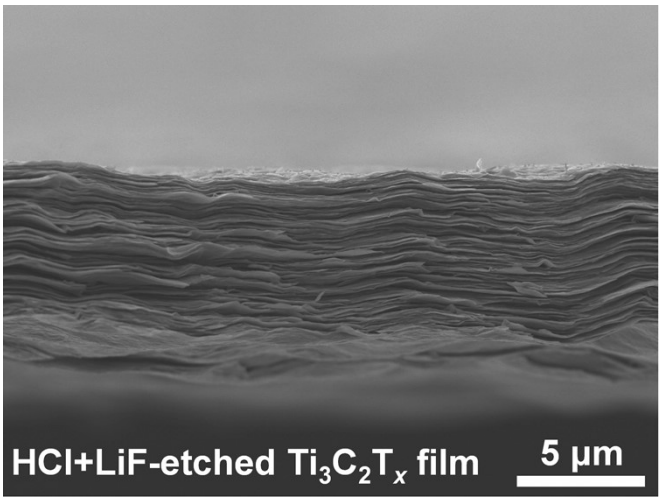

Fig. S1 Cross-section SEM image of the vacuum-filtered film from HCl+LiF-etched $Ti_3C_2T_x$ few-layer colloidal solution.

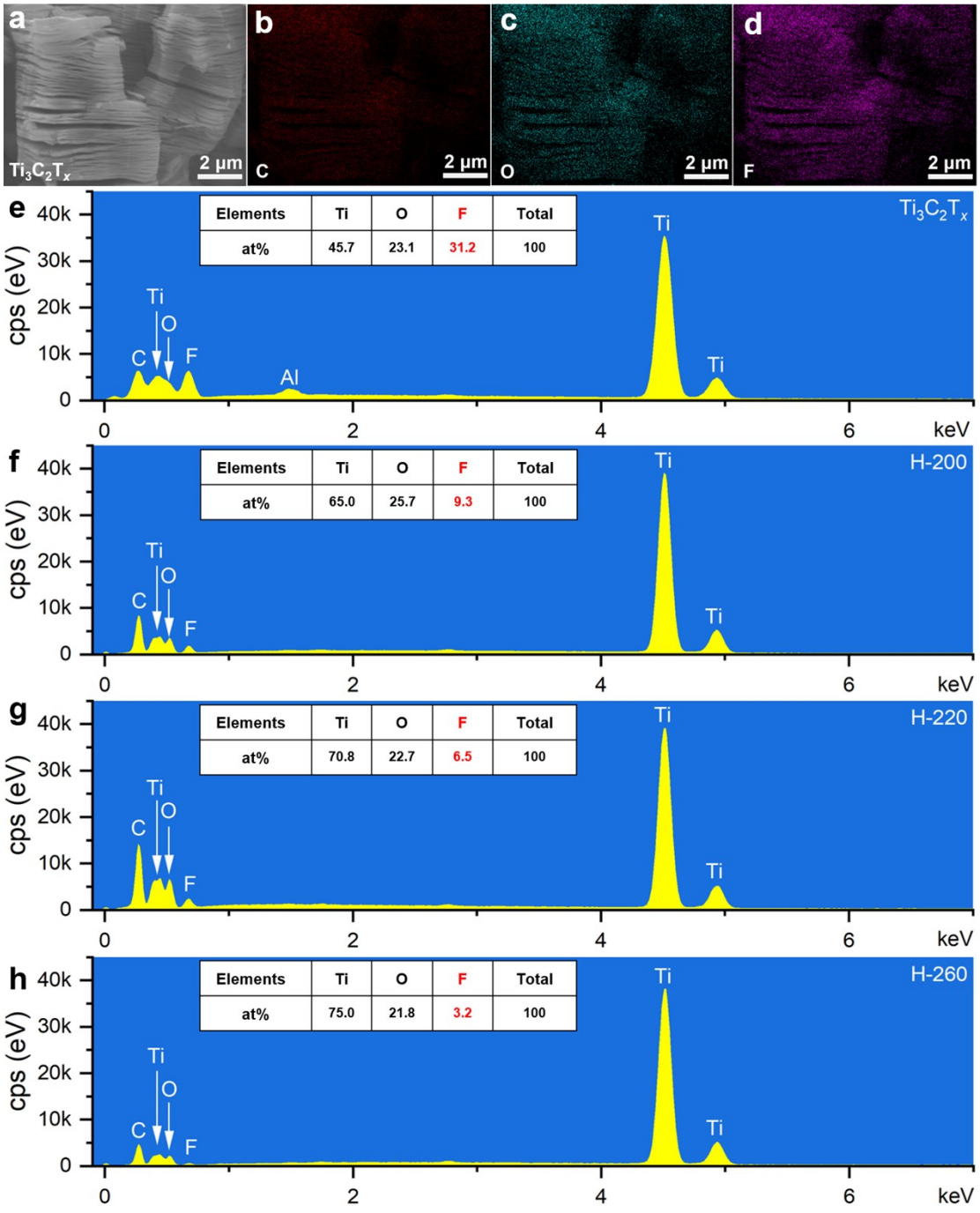

Fig. S2 (a-d) EDS element mappings and analysis of HF-etched $Ti_3C_2T_x$. EDS data of (e) the pristine HF-etched $Ti_3C_2T_x$, (f) H-200, (g) H-220, and (h) H-260.

In the pristine HF-etched $Ti_3C_2T_x$, the ratio of F+O to Ti (surface) is calculated as (31.2+23.1*0.825) / (45.7*2/3) = 1.650

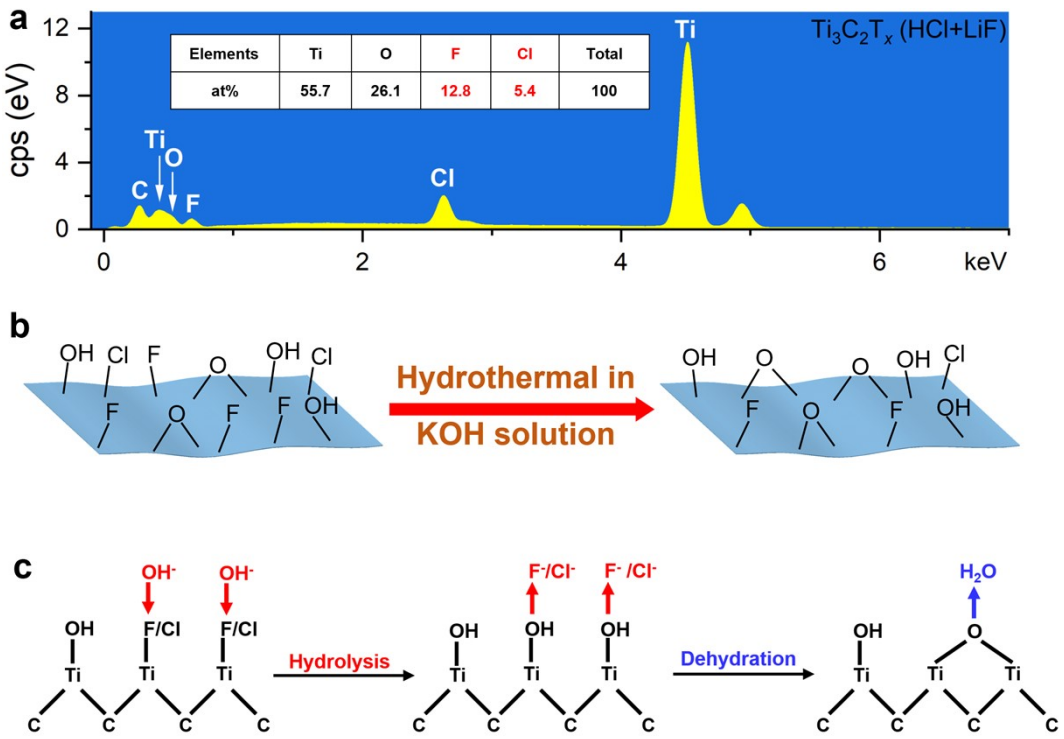

Fig. S3 (a) EDS data of HCl+LiF-etched $Ti_3C_2T_x$ vacuum-filtered film. (b) Synthesis of the HCl+LiF-etched MXene by hydrothermal treatment in KOH solution. (c) Mechanism of nucleophilic hydrolysis of halogen functional groups and dehydration.

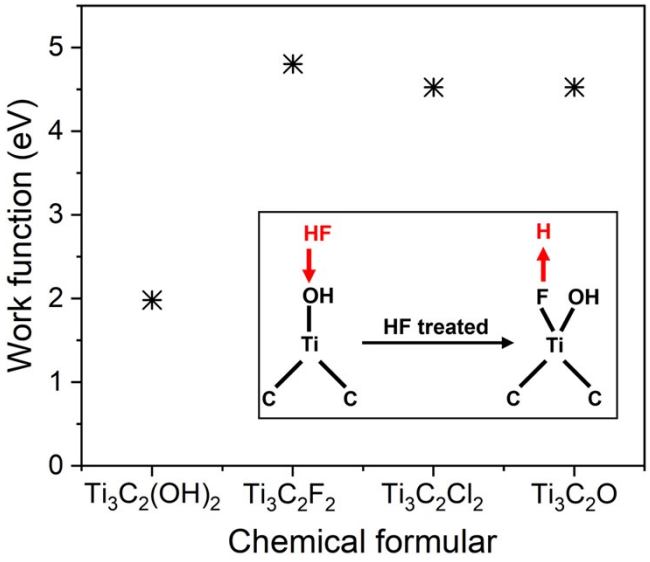

Fig. S4 Work function of Ti_3C_2 with different terminal groups. The inset shows the equation of the oxidation of trivalent titanium with hydroxyl terminal group.

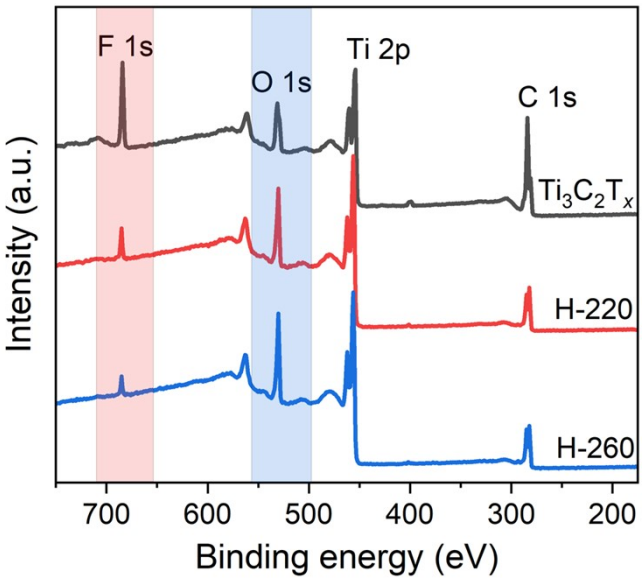

Fig. S5 XPS spectra of the pristine HF-etched $Ti_3C_2T_x$, H-220, and H-260.

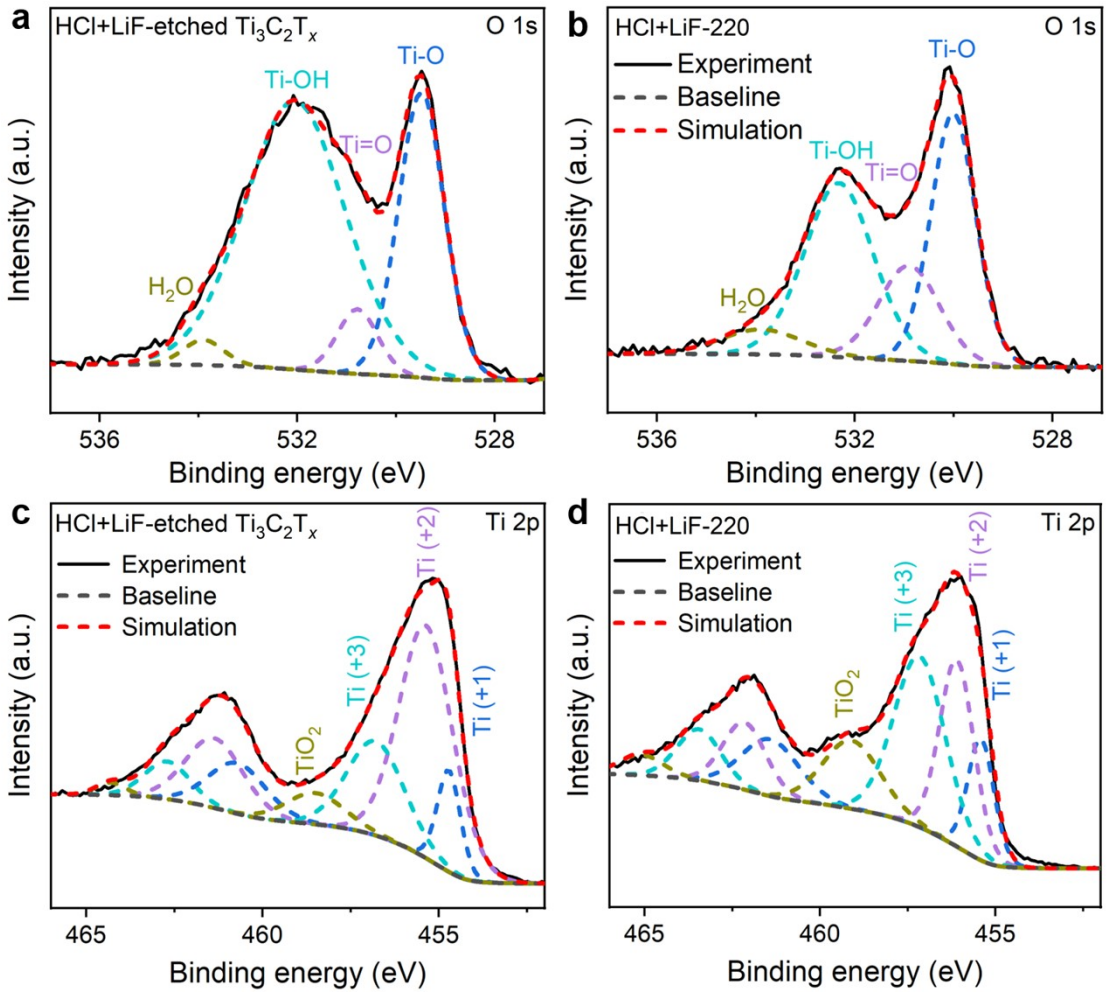

Fig. S6 High-resolution (a,b) O 1s and (c,d) Ti 2p spectra of HCl+LiF-etched $Ti_3C_2T_x$ and HCl+LiF-220.

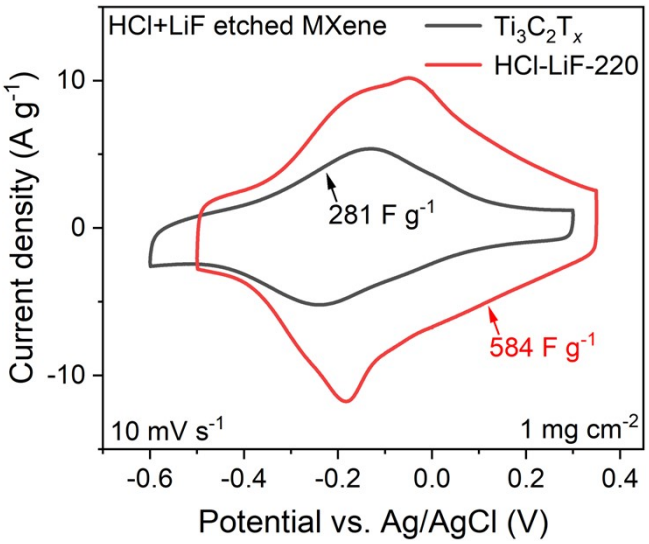

Fig. S7 CV curves of the pristine HCl+LiF-etched $Ti_3C_2T_x$ and HCl-LiF-220 with mass loading of 1 mg cm^{-2} measured at a scan rate of 10 mV s^{-1}.

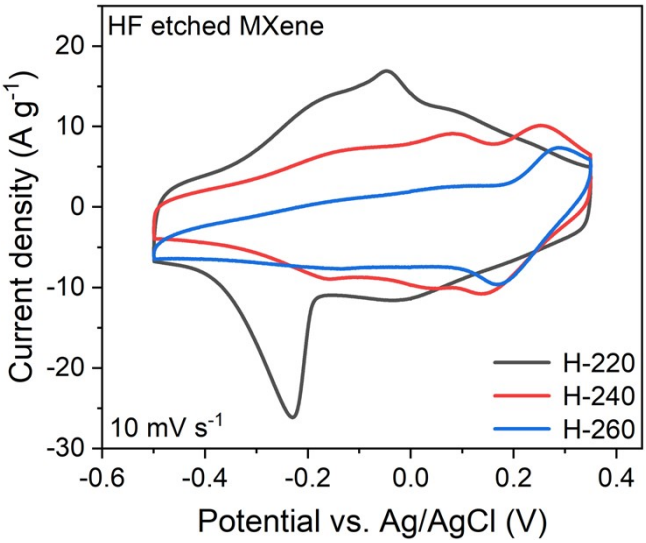

Fig. S8 CV curves of H-220, H-240, and H-260 with mass loading of 4 mg cm^{-2} measured at a scan rate of 10 mV s^{-1}.

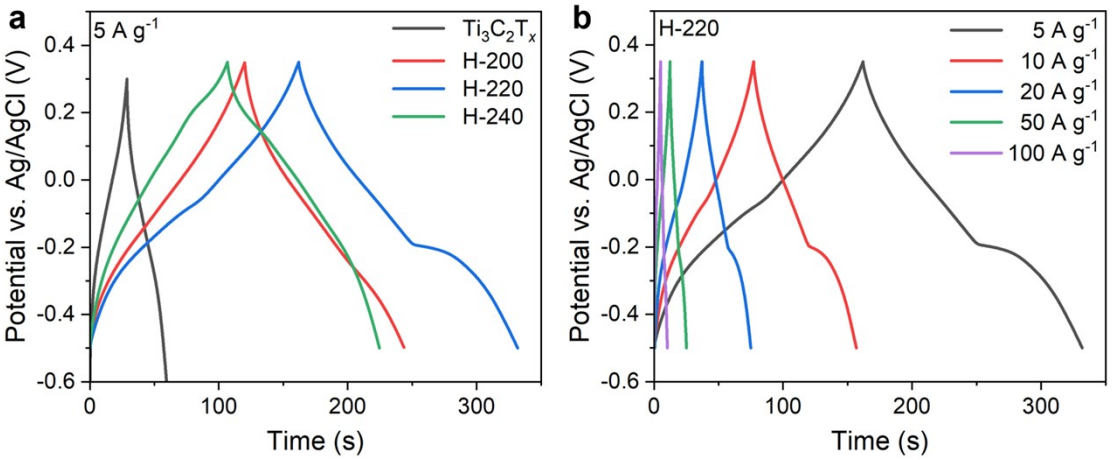

Fig. S9 (a) Galvanostatic charge/discharge (GCD) curves of pristine $Ti_3C_2T_x$ and samples hydrothermally treated in KOH solution at different temperatures at a current density of 5 A g^{-1}. (b) GCD curves of H-220 at 5, 10, 20, 50, and 100 A g^{-1}, respectively.

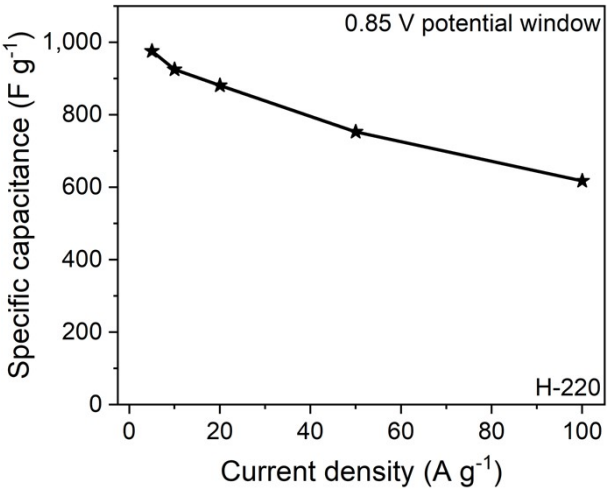

Fig. 10 Gravimetric rate performance of H-220 calculated from GCD measurements.

Similar to the results measured from CV curves, excellent rate performance is further validated by GCD tests. Even at a high current density of 100 A g^{-1}, the specific capacitance of H-220 can reach 619 F g^{-1}.

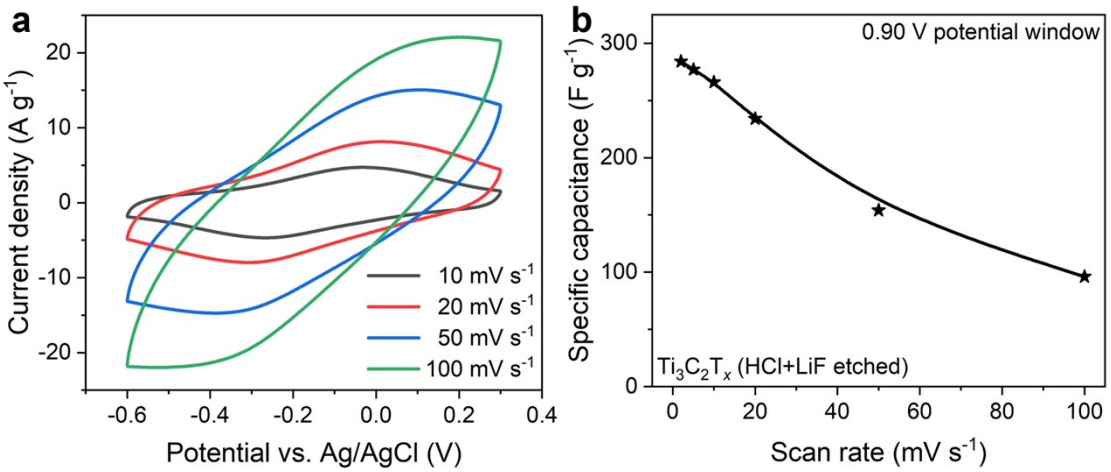

Fig. S11 (a) CV curves and (b) specific capacitances of the pristine HCl+LiF-etched $Ti_3C_2T_x$ with mass loading of 4 mg cm^{-2} measured at different scan rates.

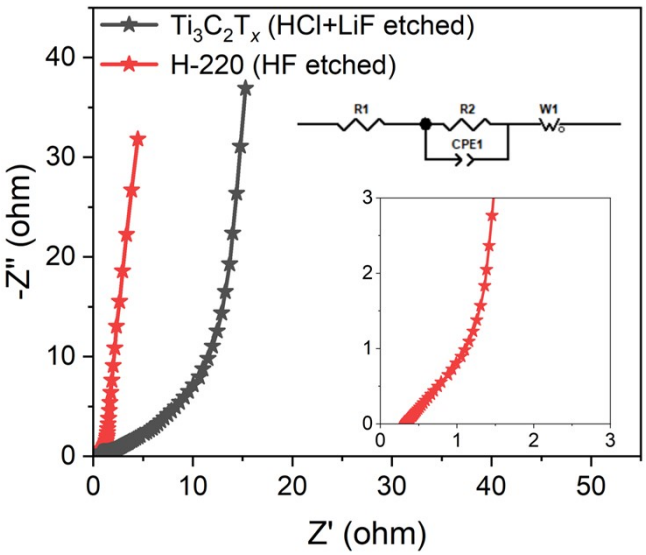

Fig. S12 Electrochemical impedance spectroscopy data collected at 0.2 V for the pristine HCl+LiF-etched $Ti_3C_2T_x$ film and H-220 electrode. Both electrodes have mass loading of 4 mg cm^{-2}.

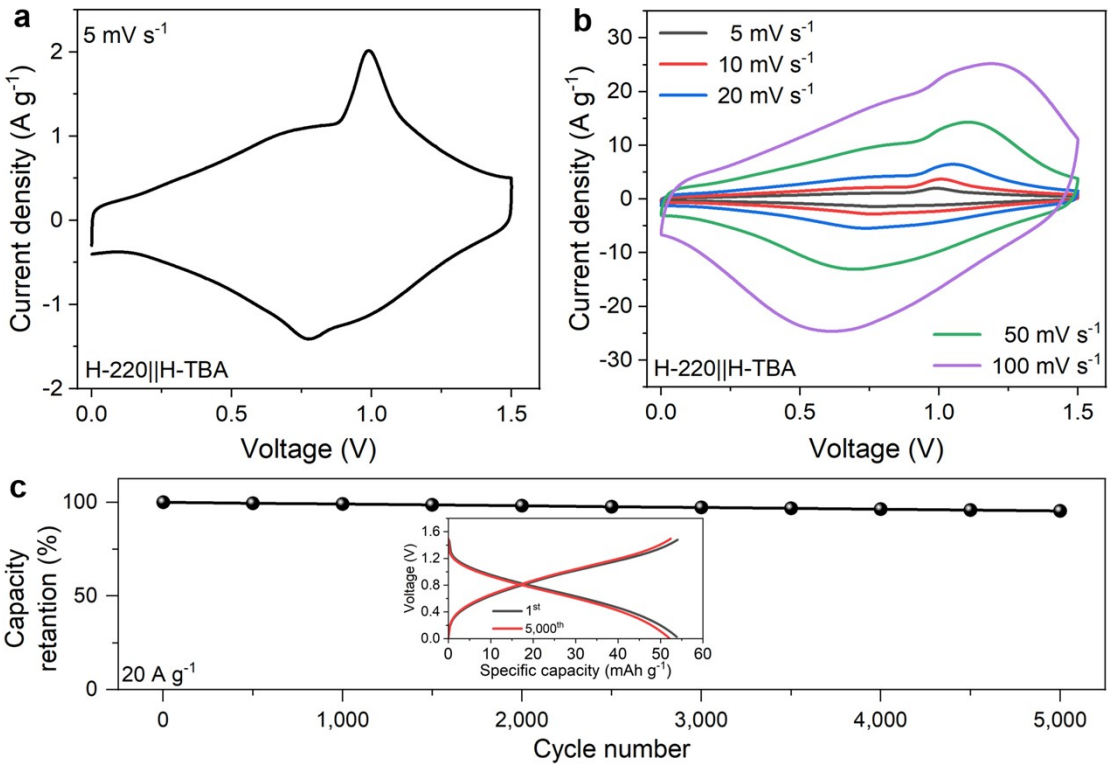

Fig. S13 (a) CV curve of H-220||H-TBA battery measured at 5 mV s^{-1}. (b) CV curves of H-220||H-TBA battery measured at different scan rates. (c) Galvanostatic cycling performance of H-220||H-TBA proton battery. The inset of (c) shows galvanostatic charge-discharge curves of the first and 5,000th cycles measured at 20 A g^{-1}.

Tables

Table S1 Percentage distribution of oxygen from XPS test.

	H_2O (%)	Ti-OH (%)	Ti-O (%)	Ti=O (%)
Pristine	17.5	63.1	17.9	1.5
H-220	8.3	17.4	44.8	29.5
H-260	10.3	12.3	44.6	32.8

Because -F terminal group is easily hydrolyzed in alkaline aqueous electrolyte, the residual -F terminal groups are mainly in the form of Ti-F. Based on the data of EDS and XPS, the ratio of Ti-O/=O to Ti (surface) can be estimated as follows: (70.8*2/3-6.5)*[(44.8%+29.5%)/(100%-8.3%)]/(70.8*2/3)=69.8%.

According to the above analysis, the terminal groups of the H-220 are mainly in the form of Ti-O/Ti=O. To facilitate the theoretical specific pseudo-capacitance calculations, we estimate the formula of H-220 as $Ti_3C_2O_y$ ($1 \le y \le 2$). Thus, the theoretical capacity (Q_p, C g^{-1}) contributed by pseudo-capacitance can be calculated as follows: $Q_p = nF/W$.

Where n is the valence number (n=2), F is the Faraday's constant (96485 C mol^{-1}), and W is the molar weight (199.63 and 183.63 g/mol for $Ti_3C_2O_2$ and Ti_3C_2O, respectively). The theoretical capacities of $Ti_3C_2O_2$ and Ti_3C_2O are 967 and 1051 C g^{-1}, respectively (2*96485/199.63=967). They can be converted to the specific pseudo-capacitance using the following equation: Q_p*ratio of active sites/potential window. So the specific pseudo-capacitance of the H-220 is in the range of 794 to 863 F g^{-1} (967*0.698/0.85=794).

Table S2 The fitted EIS data using the ZView software.

	R_1 (ohm)	R_2 (ohm)	W_1 (ohm)
Pristine	0.40	0.86	21.75
H-220	0.33	0.03	3.99

References

S1 X. Chen, Y. Zhu, M. Zhang, J. Sui, W. Peng, Y. Li, G. Zhang, F. Zhang, X. Fan, *ACS Nano*, 2019, **13**, 9449–9456.

S2 J. Xu, X. Hu, X. Wang, X. Wang, Y. Ju, S. Ge, X. Lu, J. Ding, N. Yuan, Y. Gogotsi, *Energy Storage Mater*. 2020, **33**, 382–389.

S3 Y. Dong, Z.-S. Wu, S. Zheng, X. Wang, J. Qin, S. Wang, X. Shi, X. Bao, *ACS Nano* 2017, **11**, 4792–4800.

S4 S. Zheng, J. Ma, K. Fang, S. Li, J. Qin, Y. Li, J. Wang, L. Zhang, F. Zhou, F. Liu, K. Wang, Z.-S. Wu, *Adv. Energy Mater*. 2021, **11**, 2003835.

S5 H. Jiang, W. Shin, L. Ma, J. J. Hong, Z. Wei, Y. Liu, S. Zhang, X. Wu, Y. Xu, Q. Guo, M. A. Subramanian, W. F. Stickle, T. Wu, J. Lu, X. Ji, *Adv. Energy Mater.* 2020, **10**, 2000968.